Proceedings of the 3rd Croatian Conference on Earthquake Engineering - 3CroCEE
19–22 March 2025, Split, Croatia

DOI: https://doi.org/10.5592/CO/3CroCEE.2025.45

PREDICTION OF MODAL FEATURES FOR DIFFERENT DAMAGE STAGES AND RETROFIT METHODS OF A MASONRY BUILDING

Maja Baniček [(1)], Mahmoud Shaqfa [(2)], Sara Vaing [(3)], Josip Atalić [(4)]

[(1)] *Postdoctoral Researcher, Croatian Centre for Earthquake Engineering, University of Zagreb, mbanicek@grad.hr*
[(2)] *Senior Scientist, Croatian Centre for Earthquake Engineering, University of Zagreb, mshaqfa@grad.hr*
[(3)] *PhD Student, Croatian Centre for Earthquake Engineering, University of Zagreb, svaing@grad.hr*
[(4)] *Professor, Department of Engineering Mechanics, Faculty of Civil Engineering, University of Zagreb, atalic@grad.hr*

Abstract

Under seismic and gravity loads, existing unreinforced masonry (URM) cultural heritage buildings are vulnerable and prone to damage. With careful calibration and thorough validation, credible results can be obtained from numerical tools, but this process requires reliable experimental data. Therefore, various blind prediction contests have been held recently. This paper discusses the results of a blind prediction contest of a two-story URM building that consists of a masonry vault above the ground floor and timber floor above the first floor. This contest was launched in 2023 under the DETECT-AGING project to test the damage detection capabilities of the (Structural Health Monitoring) SHM system and the reliability of numerical tools.

After generating the macro-model of the URM building, we used the implicit finite element (FEM) scheme to test the model using Abaqus software. Parametric analyses were held to calibrate key parameters of the numerical model, such as the activation and deactivation of installed steel anchors and horizontal ties, stiffness of the orthotropic timber material and the material parameters of the Concrete Damage Plasticity (CDP) model for masonry. This calibration was held following the experimental data provided included in the published competition documentation. The results of the numerical model represent the submitted prediction sheet. In general, the numerical results showed differences in modal shapes and frequencies compared to a reference state with a significant change in the damaged states.

Keywords: masonry, numerical modelling, modal parameters, non-invasive retrofitting methods

1. Introduction

Unreinforced masonry (URM) buildings and cultural heritage are vulnerable to seismic and vertical loads. While significant attention has been given to the seismic vulnerability of URM structures, less focus is on damage from aging, degradation, and soil settlement [1]. Retrofitting for seismic and vertical resilience includes invasive and non-invasive techniques. Invasive methods are time and cost-intensive, whereas non-invasive options are more economical, preventive, and often allow residents to stay in place [2]. Non-invasive methods use fiber-reinforced polymers (FRP), fabric-reinforced cementitious (FRCM) systems, and steel ties or anchors to enhance structural performance with minimal changes in the structure itself.

Engineers have tailored numerical tools and multiple methodologies to assess the performance of damaged structures and the impact of non-invasive retrofitting approaches on existing URM buildings. (maybe add examples with REFs). With careful calibration, credible results can be obtained from numerical tools, however, this process requires reliable experimental data for validation. During the last two decades, various blind prediction contests and experiments have been held to obtain reliable experimental data to test different approaches for numerical modelling of URM structures. One of the recent examples of shake table tests of a full-scale stone masonry structure was performed at the EUCENTRE laboratory [3], where the strengthening methods were applied to the structure in the mean of steel ties, steel ring beam and extra layer of planks to study the influence of the retrofit on the structure response during the seismic loading. More recently, another blind prediction contest of shake table test of a stone masonry aggregate buildings [4] were conducted. The latter contest focused on

DOI: https://doi.org/10.5592/CO/3CroCEE.2025.45

assessing the strengthening strategies applied upon significantly damaged building unit via anchoring the timber beams to the walls to prevent out-of-plane failure.

To test different approaches for numerical modelling of a URM structure in a different stages of non-invasive retrofit and damage, four Italian universities (Bologna, Genoa, Napoli Federico II, and Perugia) have launched a blind prediction contest in 2023 as part of the DETECT-AGING (Degradation Effects on sTructural safEty of Cultural heriTAGe constructions through simulation and health monitoring) project to test the damage detection capabilities of the SHM system and the reliability of different types of numerical models [5]. For the blind prediction test, a two-story masonry building was built, consisting of a single room with a masonry barrel vault above the ground floor and a wooden floor above the first floor. Measurements were carried out using the hybrid SHM system based on vibration measurements (with accelerometers) and strain measurements (with a smart brick system).

In our research, for building the model of the structure we used macro-modelling approach, where masonry is modelled as continuum with 3D solid elements. A series of sensitivity analyses were performed to calibrate key parameters of the numerical model, such as the wall-to-wall connection by tensioning steel anchors, activation and deactivation of the horizontal steel ties, stiffness parameters of the timber floor and parameters of CDP (Concrete Damage Plasticity) material model for masonry walls and vaults, by comparing experimental data included in the published competition documentation.

2. Geometry of the structure and structural elements

As a sample of the blind prediction, a two-story full-scale masonry building was built, with main dimensions of the building footprint measured 4.72 m by 3.50 m, and its total height was 4.67 m. The structure incorporates a single chamber with a masonry barrel vault of thickness 12 cm above the ground level and a wooden floor at the first level (Fig 1). The timber floor on the first floor is made of wooden planks of thickness 50 mm nailed to wooden beams of dimensions of 200 mm × 280 mm × 3250 mm supported by masonry walls A and C. Above each door or window opening, wooden lintel beams were installed with cross sectional dimensions 250 × 100 mm.

While walls A, B, and C collectively form a structural connected part of the structure, wall B is initially structurally separated from walls A, B and C and is subsequently joined to the other walls using 18 tensioned anchors on each vertical side of the wall B to ensure structural integrity. Additionally, above the ground floor, four steel ties were installed during the construction of the building connecting walls A and C.

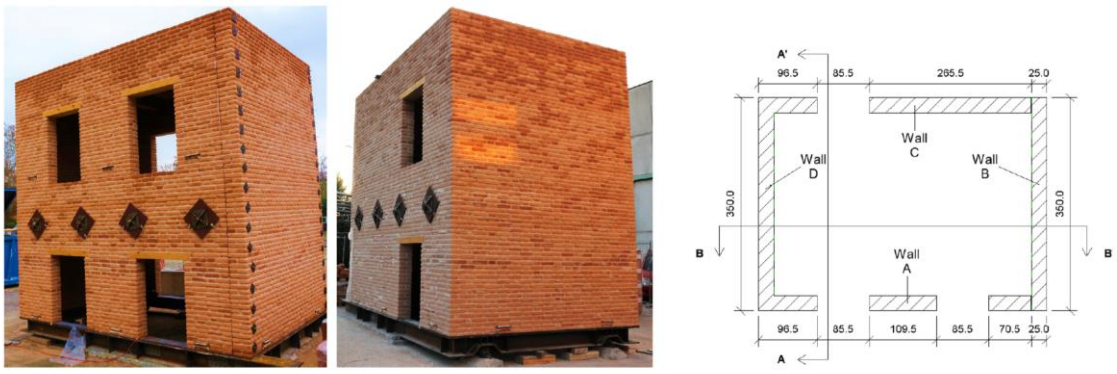

a. b.

Figure 1. a) The real constructed a full-scale URM structure; b) footprint of the model

3. Numerical model

To construct the geometry of a detailed numerical model incorporating all structural components, we utilized the Computer-Aided Design (CAD) tool Rhino [6] alongside a visual script developed in Grasshopper [7]. For numerical modeling and analysis, we employed the Computer-Aided Engineering (CAE) software ABAQUS [8]. A flowchart illustrating the process of generating a numerical model of

DOI: https://doi.org/10.5592/CO/3CroCEE.2025.45

the structure is illustrated in Fig 2. The numerical model was developed in phases, corresponding to the six experimental cases, as outlined below:

Case A: Initial Configuration. The referent model represents a masonry building consisting of three structurally connected walls (A-D-C) and one structurally separated wall (B). In this configuration, wall B is strongly connected to walls A and C via anchors applying 14 kN of force per connection. All steel ties are pre-installed during the construction phase and activated in case A. The structure includes a barrel-vaulted masonry ceiling above the ground floor and a wooden floor system composed of beams and a single layer of wooden planks at the upper level. Additionally, gravel and concrete blocks are assigned as additional mass loads on the vault and timber floor in all simulated cases.

Case B: Weak connection simulation. In this case, the anchor connections between walls B and A-C are released, reducing the force in each anchor to 0 kN to simulate weak connections.

Case C: Stiffened wooden floor. The upper-level wooden floor is reinforced by adding a second layer of wooden planks placed perpendicular to the original layer, enhancing its stiffness.

Case D: Reduced floor stiffness and tie release. This case reverts Case C floor stiffening by removing the second plank layer and releasing two middle steel ties.

Case E: Mortar removal simulation. 2.5 cm of mortar is removed from both the inner and outer surfaces of masonry walls A and C, up to a height of one meter from the base, simulating degradation or intentional material reduction.

Case F: Foundation settlement simulation. A 10 mm foundation settlement is introduced beneath wall D to assess structural response to differential settlement.

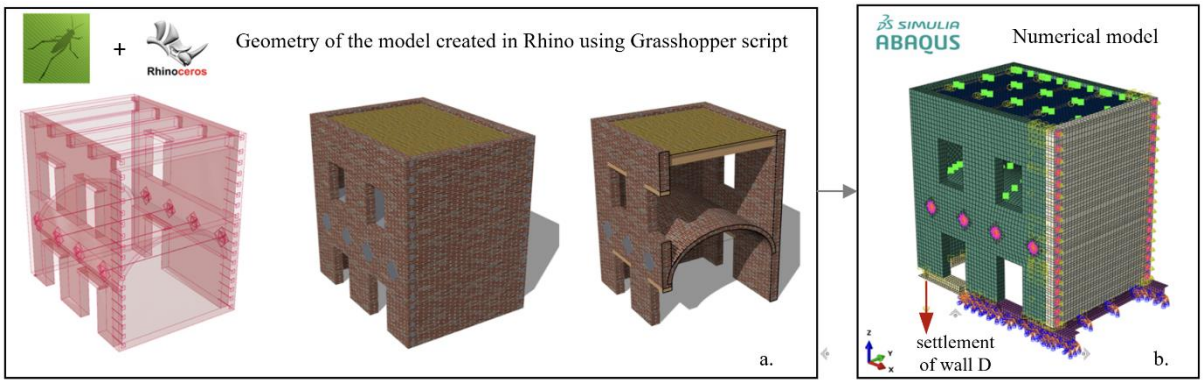

Figure 2. a) 3D view of Grasshopper and Rhino model with a cross section; b) numerical model

3.1.Loads

The model accounted for self-weight, incorporated as mass density, and additional gravel and concrete block loads applied to the vault and wooden floor. Tensile forces of 14 kN per anchor ensured structural integrity of wall B with walls A and C. Furthermore, tension bolt forces were applied to activate all four steel ties connecting walls A and C. In Case F, the foundation settlement beneath wall D was introduced by imposing a 10 mm displacement on the steel foundation beams, simulating ground movement effects.

3.2. Material properties

The numerical model incorporates steel for anchors, ties, and foundation beams, while timber is used for lintels and wooden beams, assuming isotropic mechanical properties. The timber planks above the first floor are modeled as an orthotropic shell, accounting for different stiffness values in the two principal orthogonal directions. In Case C, the thickness and mechanical properties of the wooden floor are modified during later analysis steps to simulate the installation of an additional plank layer oriented orthogonally to the first layer.

DOI: https://doi.org/10.5592/CO/3CroCEE.2025.45

For modelling of masonry material for walls and vault in ABAQUS, we utilized the Concrete Damage Plasticity (CDP) model [9]. The material properties were calibrated through parametric analysis, using experimental data to fine-tune the CDP parameters. To streamline this process, we developed a visual script in Grasshopper, allowing for interactive modification of the material properties within the ABAQUS numerical model. This approach significantly enhanced the efficiency of the calibration process. The mechanical properties of the masonry material were determined through vertical and diagonal compression tests [5], resulting in average values listed in Table 1. The material model was first calibrated using compression test data, followed by diagonal test data validation. The results of the final calibrated model for both test simulations are presented in Fig. 3a and Fig. 3b.

Table 1. Elastic properties of masonry material

Parameters	***fc* [MPa]**	**E [MPa]**	**ν (-)**	***ft* [MPa]**
Values	8.33	2976	0.34	0.21

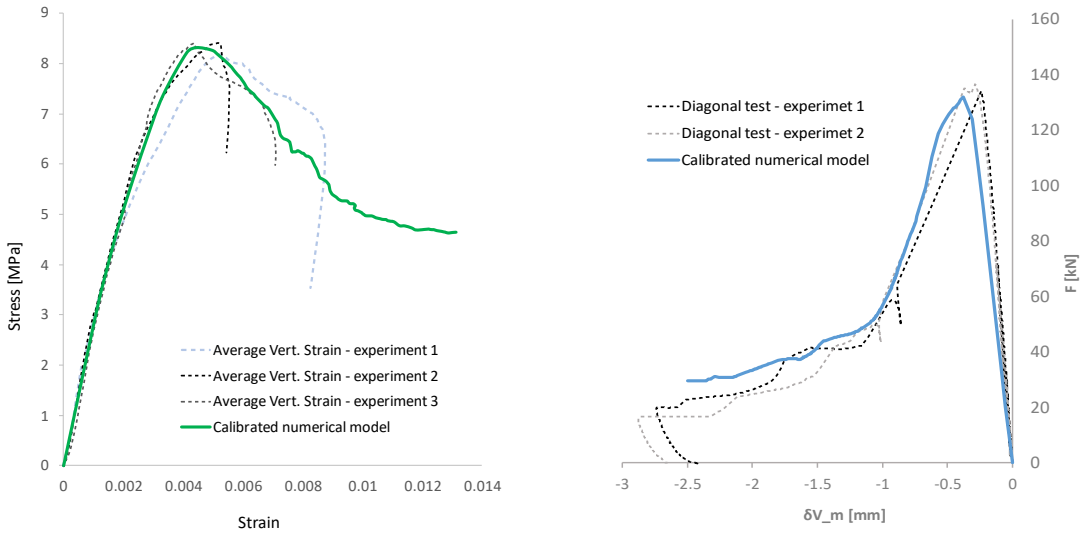

a. b.

Figure 3. Numerical simulations of experiments: a) compression test (stress-strain), b) diagonal compression test (force- relative vertical displacement of speciment)

4. Analysis and results

Figure 4 presents a comparative analysis of the frequencies corresponding to the first five significant modes across all six cases. As observed, the most significant frequency shifts occur in Cases B and F, which is expected, as both scenarios simulate structural damage. Case B represents a weak vertical wall-to-wall connection between wall B and the rest of the structure, significantly reducing the global stiffness of the structure and leading to notable frequency changes. Case F simulates foundation settlement beneath wall D, inducing structural deformations and further altering the modal characteristics. In contrast, Cases C, D, and E, which involve non-invasive strengthening methods, exhibit no significant frequency variations in the first four modes. However, a slight increase in frequency is observed in the fifth mode, indicating a minor influence of these modifications on the higher-order dynamic response of the structure.

DOI: https://doi.org/10.5592/CO/3CroCEE.2025.45

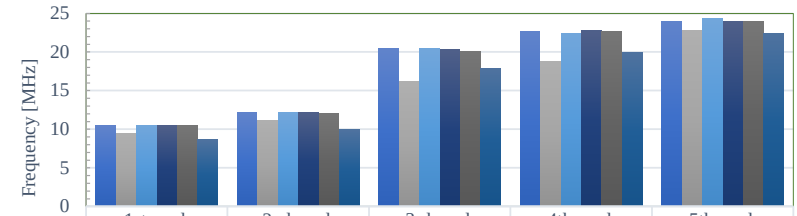

	1st mode	2nd mode	3rd mode	4th mode	5th mode
Case A	10.511	12.163	20.388	22.63	24.02
Case B	9.434	11.182	16.12	18.811	22.804
Case C	10.542	12.205	20.416	22.462	24.375
Case D	10.511	12.147	20.324	22.794	24.011
Case E	10.464	12.009	20.137	22.606	23.884
Case F	8.727	10.011	17.812	19.888	22.415

Figure 4. Values of frequencies that correspond for each mode and case

To better understand the changes in modal shapes between a case with a good (Case A) and a poor (Case B) wall-to-wall connection, we compared the modal displacements of the first three modes, as shown in Figure 5. The differences between these modal shapes are further visualized in Figure 6.

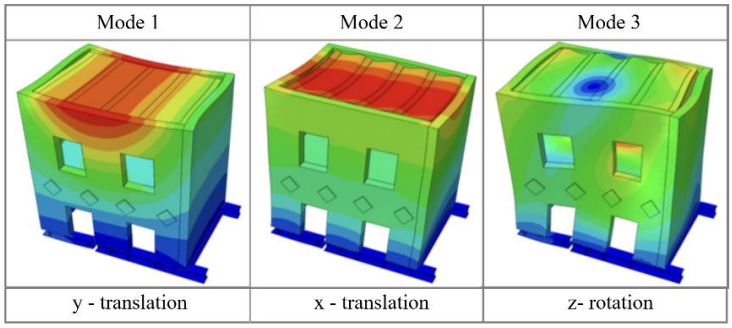

Figure 5. First three modal shapes for the difference in displacements between case "A" and "B"

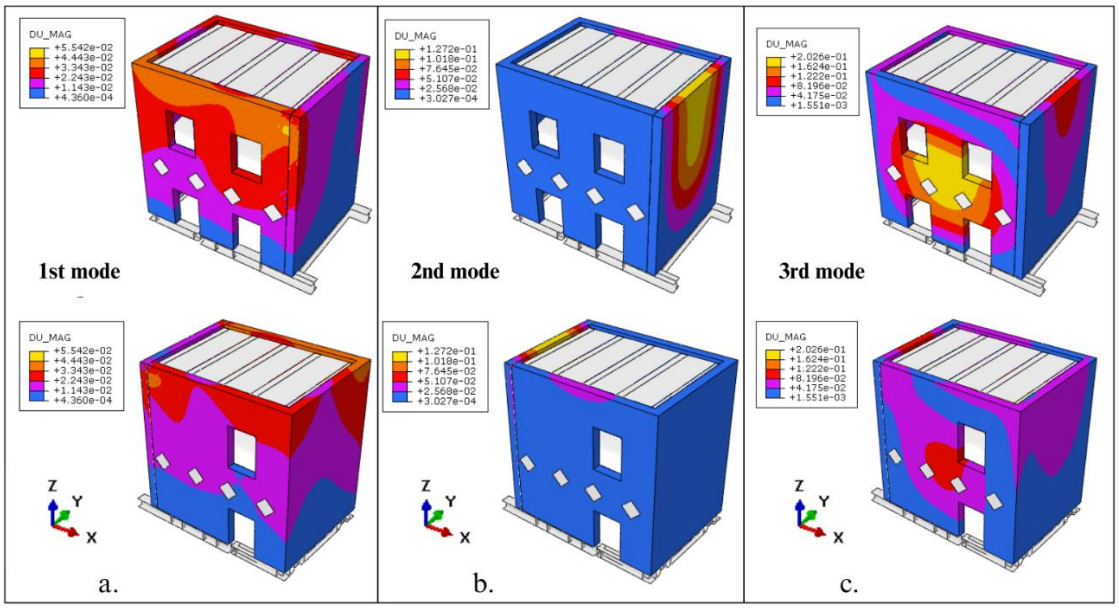

Figure 6. 3D visualization of differences in displacement of the first three modal shapes: between case "A" and "B": a) in y – displacement, b) x – displacement and c) z - rotation

DOI: https://doi.org/10.5592/CO/3CroCEE.2025.45

5. Conclusion and future work

The results obtained with the numerical model showed differences in modal shapes and frequencies compared to a referent case "A" with a significant change in the damaged states "B" and "F". The cases with applied non-invasive retrofit methods did not show significant change in the frequencies, but these methods are crucial for out-of-plane.

This study is of a significant value for the Croatian engineering community as nearly all the constructed buildings in the historical center of Zagreb Downtown are URM structures Such structures are known for their high vulnerability to seismic activity, a fact highlighted by the recent 2020 earthquakes in central Croatia. These buildings, predominantly constructed in the late 19th and early 20th centuries, exhibit weak structural integrity between walls and floors. While the objective of the blind prediction competition was to assess damage accumulation from ageing, degradation, and soil settlement, the findings could also substantially contribute to numerical models for cost-effective, preventive and non-invasive retrofitting strategies for existing URM buildings against earthquake impacts in Zagreb Downtown.

For the future, we envisage working on first cross validating the current findings with other beam element models. Next, we will compare our results with the experimental findings and work on a post-diction paper. In that paper, we will use evolutionary algorithms (ES) to auto-calibrate our material properties and see how close we can get to the experimental results and the current numerical ones. The latter will also shed light on the reliability and trust of current engineering practices using commercial numerical software.

Acknowledgements

This research was funded by the Croatian Centre for Earthquake Engineering and Croatian Ministry of Science, Education and Youth, grant number A679117 – HPC – Research project in the field of Earthquake Engineering.

References

[1] Ertürk Atmaca, E., Genç, A. F., Altunişik, A. C., Günaydin, M., & Sevim, B. (2023). Numerical Simulation of Severe Damage to a Historical Masonry Building by Soil Settlement. *Buildings*, *13*(8), 1973. https://doi.org/10.3390/buildings13081973

[2] Dizhur, D., Ismail, N., Knox, C., Lumantarna, R., & Ingham, J. M. (2010). Performance of unreinforced and retrofitted masonry buildings during the 2010 Darfield earthquake. *Bulletin of the New Zealand Society for Earthquake Engineering*, *43*(4), 321–339. https://doi.org/10.5459/bnzsee.43.4.321-339

[3] Guerrini, G., Senaldi, I., Graziotti, F., Magenes, G., Beyer, K., & Penna, A. (2019). Shake-Table Test of a Strengthened Stone Masonry Building Aggregate with Flexible Diaphragms. *International Journal of Architectural Heritage*, *13*(7), 1078–1097. https://doi.org/10.1080/15583058.2019.1635661

[4] Tomić, I., Penna, A., DeJong, M. *et al.* (2024). Shake table testing of a half-scale stone masonry building aggregate. *Bull Earthquake Eng* **22**, 5963–5991. https://doi.org/10.1007/s10518-023-01810-y

[5] N. Buratti, S. Cattari, G. Lignola, A. Meoni, F. Parisi, F. Ubertini & G. Virgulto (2023). DETECT-AGING blind prediction contest: a benchmark for structural health monitoring of masonry buildings, *Procedia Structural Integrity*, 44, 2128-2135, doi: https://doi.org/10.1016/j.prostr.2023.01.272.

[6] R. McNeel and Associates: *Rhinoceros 3D*, www.rhino3d.com, 15.1.2024

[7] R. McNeel and Associates: *Grasshopper 3D*, www.grasshopper3d.com, 15.1.2024

[8] Dassault Systèmes: SIMULIA, User Assistance 2020, 2020.

[9] Lubliner, J., Oliver, J., Oller, S., & Oñate, E. (1989). A plastic-damage model for concrete. *International Journal of Solids and Structures*, 25(3), 299-326.